IOP Conf. Series: Materials Science and Engineering **1345** (2026) 012001 doi:10.1088/1757-899X/1345/1/012001

First Approximation for Unified Fatigue Models for 316 Stainless Steel and IN718 Materials at 4K, 77K & 293K from Monotonic Material Properties

Michael D. Marotta[1*], R. Keith Kersey[2], Agnieszka Wusatowska-Sarnek[3], Taylor Pratt[4], Andreas Kulovits[5], Claire Saunders[6]

[1, 2] Advanced Fracture Mechanics Associates LLC, Lebanon, CT, United States
[3, 4, 5, 6] Commonwealth Fusion Systems, Devens, MA, United States

[*]E-mail: mdm@adv-fma.com

Abstract. Fusion applications require the use of materials that are capable of withstanding the cyclic electromagnetic forces of toroidal field coils during start-up and shutdown at cryogenic temperatures. Because of the cyclic nature of loading, a low cycle fatigue (LCF) model is essential to determine operational life and prevent premature failure. Thus, there is a need for test data at low temperatures, specifically at 77K and 4K, corresponding to the temperatures of liquid nitrogen and helium. However, testing at such conditions is expensive, requiring proper containment, sufficient coolant supply, and control monitoring. Thus, the initial approach was to establish a foundation of available fatigue data, then supplementing the database with additional testing as needed. At this time, the data from the literature search has been successfully fit at three temperatures (4K, 77K, 293K) to a Manson-Coffin-Basquin model with a 50 % (typical) to 0.1% probability-of-failure scatter factor of 3.85. Additional work has been done to apply this data to a hardness-based lifing approach, which proposes that fatigue behavior can be approximated using monotonic properties. Preliminary results have been successful for 316 stainless steel and Inconel 718, resulting in conservative but reasonable estimates for both room and cryogenic temperatures.

1. Introduction

Stainless steel grade 316 is an austenitic steel that sees widespread industry use second only to Type 304. The addition of molybdenum gives it enhanced corrosion resistance, thus making it idea for harsh environments such as marine or chemical applications [1,2]. The addition of both nickel and molybdenum give it significant ductility and crack resistance during forming while its ability to retain both strength and corrosion resistance during welding gives it excellent weldability [3]. Type 316 steel is generally more difficult to machine than 304 due to the tendency of the former to strain harden through cold working. The heat treatment process for 316 stainless begins with solution annealing at a temperature range of 1,040°C – 1,120°C (1,900°F – 2,050°F). It then undergoes rapid cooling via water quench such that ideal mechanical properties and corrosion resistance are retained. After this stage, any additional strength can only be imparted to the material by way of cold working [1,3].

There are several variants of 316 steel that were evaluated in this program. The first is 316L, or low carbon 316, and is used in applications where enhanced corrosion resistance is necessary

as is has a lower risk of forming carbides [2,3,4]. Type 316LN has both low carbon content and additional nitrogen, typically ranging from 0.1% to 0.3%. This has the effect of raising its minimum yield strength, enhancing creep / stress rupture capabilities, and increasing its resistance to sensitization under some circumstances [3,4,5,6,7]. However, the additional solid solution hardening makes it somewhat less ductile and thus slightly more susceptible to brittle failure than 316L [4]. This variant is prevalent in marine, chemical processing, oil and gas, and high temperature pressure applications like pressure vessels, boilers, and heat exchange units [1,2,4,6]. Type 316LNH is a subset of 316LN, in which the minimum nitrogen content is limited to 0.2% or higher. This specification is consistent with the material chemistry tested internal to Commonwealth Fusion Systems (CFS), and other sources in literature [8] that were used for model development. Unmodified 316 was not evaluated in this program.

The chemical composition of 316 and common variants described in the following section are shown in Table 1 [7].

Table 1. Typical Chemical Composition of 316 and Variants

	Content (%)			
Element	**316**	**316L**	**316LN**	**316LNH**
Iron	Balance	Balance	Balance	Balance
Chromium	16.0-18.0	16.0-18.0	17.0-19.0	17.0-19.0
Nickel	10.0-14.0	10.0-15.0	13.0-15.0	13.0-15.0
Molybdenum	2.0-3.0	2.0-3.0	2.0-3.0	2.0-3.0
Manganese	2	2	2	2
Silicon	1	1	0.75	0.75
Nitrogen	0.1	0.1	0.1-0.3	> 0.2
Phosphorous	0.045	0.045	0.25	0.25
Carbon	0.08	0.035	0.03	0.03
Sulfur	0.03	0.03	0.1	0.1

The relative strength, toughness, and fatigue / crack growth capabilities of 316 stainless steel, especially at lower temperatures, also makes it an ideal candidate for use in a number of applications within magnetic fusion energy systems. As a result, there is a significant interest in quantifying the capabilities of this material and its variants.

Modern low cycle fatigue (LCF) analysis of high stress / life limiting locations in fusion applications follows the standards set forth in the 2021 ASME VIII, Division 2 Boiler and Pressure Vessel Code [9]. The reference curve used for evaluation of low temperature 316 also applies to all 300- type steels below 700K and incorporates an adjustment factor of 20X on life or 2X in stress for design applications, whichever is more conservative.

There has been interest in transitioning to the use of a more direct “data driven” method based on first principles of fatigue analysis. Such an approach would make use of cryogenic strain and load controlled Type 316 fatigue data, resulting in a model and corresponding design curve factor that would be specifically tailored to this material. Thus, one objective of this effort is to create a model that covers low temperature fatigue ranging from near-absolute zero to room temperature data in a unified model. The development of this model uses the previous work in characterizing Inconel 718 as a foundation [10].

While fatigue data at superfluid temperatures (e.g. 4K) is limited, there were several populations available that provided sufficient basis for a model [8,11,12,13,14]. Data at higher superconducting temperatures (e.g. 77K) was more limited [13] and required additional testing

as part of this program. Room temperature data was relatively easy to find and incorporate, given its low cost and rapid turnaround time compared to lower temperature data [15,16].

In addition to the development of a unified cyclic fatigue model the limited amount of low temperature data, the high cost of testing, and the time necessary to generate results prompted a search for an alternate approach to characterizing fatigue through the use of monotonic properties. Work performed by Hartman and Glinka [20] on the correlation of fatigue life with Brinell hardness and elastic modulus will be reviewed in *Section 5.5: Evaluation of Hardness Model,* including its application to the 316 program database as well as data from previous modeling efforts [10].

2. Procedure

2.1 Material and Specimens

The initial approach for this program focused on gathering all data within the 316 specification, regardless of specific chemistry. The population was down-selected to include only the low carbon version of 316 (316L/LN/LNH) after noticing the relative differences in fatigue behavior.

All of the data used for development came from smooth and fully reversed (R = -1) round bar specimens machined from forgings or hot rolled plate material. Most were 6mm in diameter, with one source that tested 10mm bars at room temperature. One population of data did not specify the specimen dimensions [11] but are assumed to be consistent with the remainder of the database.

There were some sources that had specimen data tested at alternate stress ratios (R = 0.1), but there were outstanding questions regarding the way the material was processed by way of either initial heat treatment or subsequent cold work that they could not confidently be considered part of the same material without a population of parity data to prove it. Thus, they were left out for this program; however these may be revisited at a later time once additional data becomes available.

A summary table representing the model calibration database is shown below in Table 2, illustrating showing individual specimen counts sorted by author, material variant, dimensions (if available), control type, and temperature.

Table 2. Data and Specimen Summary

				SPECIMEN COUNT		
Source	Dimensions	Control	Chemistry	4K	77K	293K
Hamada	6mm dia	load	316LNH	16		
Nakajima	unk	load	316L	2		
Suzuki	6mm dia	strain	316L	7		
Ogata	6mm dia	strain	316LN	5	3	4
CFS (PES)	6.35mm dia	load	316LNH		12	
Strizak	5, 6.35mm dia	strain	316LN			17
Goyal	10mm dia	strain	316LN			6

2.2 Test Procedures

Fatigue tests were conducted with closed loop servohydraulic test machines with a triangular waveform. Axial strains were measured using an externally mounted extensometer for either strain control or strain measurement / monitoring under load control. Applied strain rates, if

provided, ranged between 0.1%/s and 0.4%/s to prevent an increase in specimen temperature. One source did not provide test frequency [8], but their previous work for JJ1 material specified a strain controlled test frequency of 0.2 Hz for specimens that exceeded yield and a load controlled test frequency of 10 Hz for tests in the elastic range. No such distinction was made in his work for 316LNH, so while it is possible they followed a similar protocol, it is presumed that all tests were performed under load control at a frequency of 10 Hz.

Similar to the metadata analysis performed in Inconel 718 [10], full details – including schematics and standards – of the mechanical test protocols related to each individual source are described in full in the original documentation.

3. Experimental Results

Information and details about the source and type of fatigue data used for model calibration are shown in Table 2 of the previous section. The fatigue database for low carbon 316 steel and its variants consists of three temperatures – 4K, 77K, and 293K – and is limited at this time to fully reversed (R = -1); additionally, no notched or bolthole specimens were available to determine the effects of geometry. Because of concerns about temperature increase resulting from elevated test frequency, the majority of data is also limited to low frequency / strain rate.

The majority of the database was built from data digitized from plots provided within the literature, with the exception being the data generated by CFS, which was provided in tabular format. Additionally, CFS was the only source that provided initiation life, giving some insight into the relationship between initiation and failure for 77K; however given the limited scope of this information, the model was developed based on cycles to failure.

Figure 1 shows the typical behavior of low carbon 316 fatigue at 4K. Fatigue lives span the range of 100 to 1 million cycles to failure, incorporating fully reversed data tested under both strain and load control. One interesting feature to this data is the sudden, discontinuous drop in cycles to failure after reaching a strain amplitude of approximately 1%. Instead of continuing along a power-law type trend with increasing strain, there is a noticeable flattening of the curve, suggesting a cutoff stress above which the fatigue life is effectively zero.

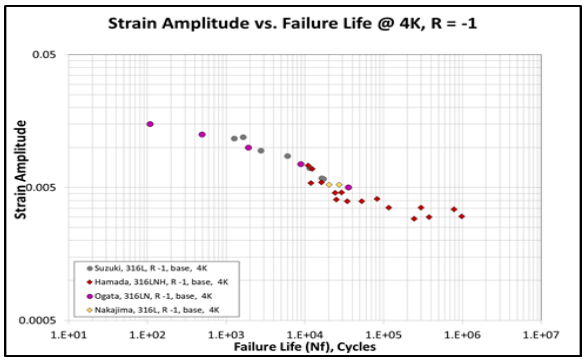

Figure 1. Strain Amplitude v. Failure Life for 316 at 4K

This stress cutoff trend can also be observed to a lesser extent at 77K (Section 5.2, Figure 4). It is unclear whether it is present to room temperature due to a lack of data at higher strain values, but concerns of anticonservatism in design led to the incorporation of the "cutoff" strain for the entire temperature range of the fatigue model (see "Analysis").

4. Analysis

4.1 Stress Strain Model

In order to properly incorporate the test conditions of load controlled fatigue data into a strain life model, the actual strain response must be calculated through the use of a constitutive model. This is done by making use of the Ramberg-Osgood formulation, which is a power law equation relating the stress and plastic strain and amplitudes observed at mid-life [17,18].

$$\sigma_a = K'\left(\varepsilon_a^p\right)^{n'} \rightarrow \varepsilon_a^p = \left(\frac{\sigma_a}{K'}\right)^{1/n'} \rightarrow \varepsilon_a = \frac{\sigma_a}{E} + \left(\frac{\sigma_a}{K'}\right)^{1/n'} \quad (1)$$

The values of σ_a, ε_a, and $\varepsilon^p{}_a$ refer to the stress, strain, and plastic strain amplitudes respectively. K' and n' are the cyclic strength coefficient and cyclic strain hardening exponent. Load controlled strain amplitude response for use in a strain-life model can be calculated directly. In the case of notched locations where neither the stress and strain states are known, this equation must be solved iteratively.

Stress-strain data was readily available in the form of mid-life plastic strain amplitudes at 77K from CFS and mid-life stress amplitude values from Goyal at room temperature [15]. Some limited data showing the evolution of maximum stress as a function of cycle count was available at 4K from Ogata [13], which was used to create an approximate model on the assumption that the stress strain response remained roughly centered around zero. This data allowed for the creation of a table of cyclic Ramberg Osgood coefficients with which the strain response of load controlled tests were calculated, as shown in Figure 2.

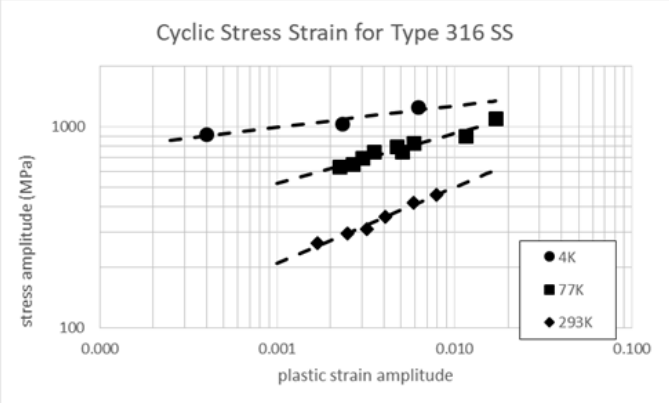

Figure 2. Cyclic Stress Strain Relationships for 4K, 77K, 293K

4.2 Fatigue Model

Fatigue behavior of Type 316 steel is best represented by the Manson Coffin Basquin formula, which is a double power law equation relating applied strain amplitude at fully reversed conditions and cycles to failure N_f [17,18]. Such a formulation is better suited for evaluating data that includes low cycle fatigue conditions where cyclic plasticity plays a dominant role in crack initiation. The term on the left is the fully reversed strain amplitude. The two coefficients, σ_f' and ε_f' are the fatigue strength and fatigue ductility coefficients, respectively. The values b and c are the stress and strain exponents, and E is the elastic modulus. Additionally, the model incorporates "cutoff" cycle count D, below which the allowable stress reaches a limit state and any value exceeding it will result in zero life. This change was incorporated in response the drop in life at

high values of applied strain as described in the previous section. Coefficients n_1, n_2 and n_3 determine the position and slope of the cutoff segment of the curve.

$$\frac{\Delta\varepsilon_{R=-1}}{2} = \frac{\sigma_f'}{E}\left(\max\left(2N_f, D\right)\right)^b + \varepsilon_f'\left(\max\left(2N_f, D\right)\right)^c \tag{2a}$$

$$D = n_1 e^{\left(-\frac{N_f}{n_3}\right)} + n_2\left(1 - e^{\left(-\frac{N_f}{n_3}\right)}\right) \tag{2b}$$

Because fatigue life is written as the independent variable, this equation must be solved iteratively by way of a pre-packaged solver or interval halving routine.

Standard model fitting was performed as part of this program, and involves generating ideal values of the four parameters by way of iterative optimization. Previous experience has shown a reasonable fit is achievable if the values of the coefficients σ_f' and ε_f' are set and subsequently fixed to the temperature-dependent ultimate tensile strength and ductility limits; this may not be true in the general case but doing so should at the least provide a practical starting point for optimization.

In addition to the standard model fitting method, another approach based on the use of monotonic tensile / hardness properties was also investigated. It is based on the work of Hartman and Glinka [20], who conducted a material parameter study of 69 varieties of steel, finding that the best overall average correlation between monotonic parameters and cyclic behavior can be represented by a function of Brinell hardness HB and the elastic modulus E as seen in Equation 3.

$$\frac{\Delta\varepsilon_{R=-1}}{2} = \frac{4.25(HB)+225}{E}\left(2N_f\right)^{-0.09} + \frac{.32(HB)^2-487(HB)+191000}{E}\left(2N_f\right)^{-0.56} \tag{3}$$

The Ramberg Osgood relations remain unaffected, but the parameters K' and n' are set by the relationship between the Manson Coffin parameters (refer to Equations 1 and 2).

$$n' = \frac{b}{c}; \qquad K' = \frac{\sigma_f}{{\varepsilon_f}^{n'}} \tag{4}$$

Such an approach could be very useful in situations where cyclic data is either limited or non-existent, and some first order approximation of fatigue behavior is needed. It would not replace a fully developed model in most cases, but would be useful in providing a guide for preliminary design or for test matrix development until a larger body of data becomes available.

5. Discussion

5.1 Results at 4K

The results of model calibration at 4K are shown in Figure 3a. Typical model fit is shown as a solid line. The minimum suggested design curve is a combination of the lowest value between the 20X life debit and 2X strain debit at a given failure life, explaining the "bumps" in the curve where one crosses over the other.

The higher life values of the fatigue data show consistency with the standard double power law form of the Manson Coffin equation. The stress-life limit transition can be seen at $N_f \sim 10{,}000$, captured well with the coefficient D. It is strongly recommended that component designs avoid loads that would result in strains that exceed this value.

Other sources [12] suggest a design approach for 4K limiting the allowable stress to 2/3 s_{yield}. This would avoid the risk of both martensitic transformation and significant serrated yielding coincident with plastic deformation at this temperature, which increases the risk of significant life shortfalls in unconstrained load controlled locations.

Figure 3b shows the 4K model calibration data elastically converted to stress, re-scaled and superimposed with data corresponding JSME design curve referenced by Nakajima, et al [11]. Representing the data this way illustrates how the new model curve is essentially identical to the JSME design curve for higher cycle counts (> 200,000), and slightly conservative down to 10,000 cycles. The incorporation of data from Suzuki and Ogata is what causes the curve to flatten below 10,000 cycles, deviating from the JSME which did not include these data sets.

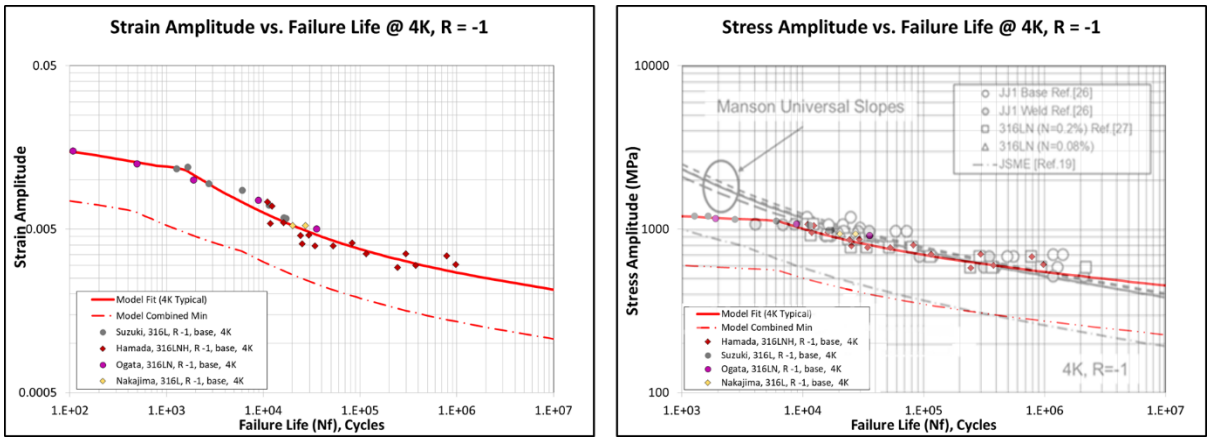

Figure 3a, b. 4K 316 Strain-Life Data with Manson Coffin Model Fit (3a, left); 4K 316 Stress-Life Plot Superimposed with JSME Fit (3b, right)

The load response of the strain controlled tests were calculated using Ramberg-Osgood coefficients taken from the Ogata strain controlled data, since it was the only source with stress strain data that had the appropriate material chemistry. While consistent with Goyal results at room temperature, it showed significant deviation from the CFS data at 77K; thus, the 4K strain controlled results should be considered preliminary until additional data can be acquired.

5.2 Results at 77K

The curve at 77K (Figure 4) is shallower than that at 4K but still follows the double power law relationship. The CFS data and the higher strain Ogata data show some level of non-conservatism relative to the typical model curve. A similar cutoff was observed at this temperature, similar to 4K but significantly less abrupt. Until additional testing is done, the cutoff term will remain at this temperature to avoid potential non-conservative results at higher stresses.

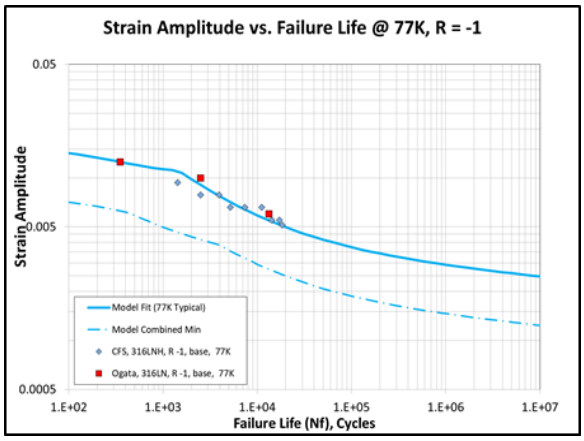

Figure 4. 77K 316 Data with Manson Coffin Model Fit

The load response of the strain controlled tests were calculated based on coefficients taken from the CFS and Botshekan data [19]. Ogata was avoided, for reasons explained in the previous section. Stress-strain response between the two groups matched well and had the same lognormal relationship resulting in a power law fit applicable to both data sets.

5.3 Results at 293K

The 293K (room temperature) curve and calibration data are shown in Figure 5. There is a substantially larger range of failure lives than other temperatures due to the relatively low cost and greater need for room temperature steel fatigue data. As with 77K, there appears to be widespread agreement among all of the data sets at higher lives. Strain controlled load response was calculated based on the cyclic stress strain curve from Goyal [15]. Limited supplemental data from Ogata and Strizak were in general agreement, thus lending confidence in their values [13,16].

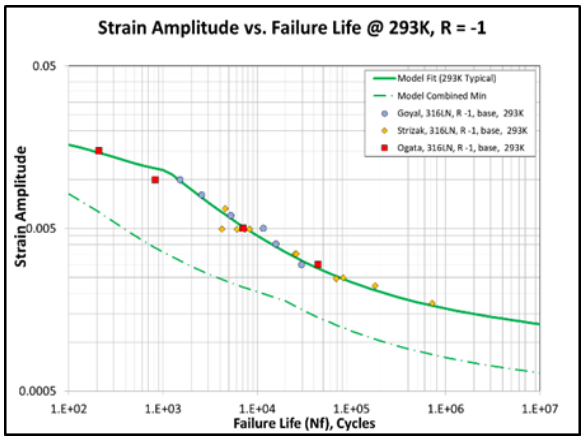

Figure 5. 293K 316 Data with Manson Coffin Model Fit

5.4 Lognormal Fit

Figure 6 shows the distribution of error for each data point in terms of actual over predicted cycles to failure (A/P). Because of the logarithmic nature of the relationship between stress / strain and failure life the corresponding error and uncertainty of the model is characterized using a normal

distribution of the base-10 log of the error (i.e. lognormal). The distribution of the error for this model, which incorporates all three temperatures of 4K, 77K, and 293K, shows that the typical to minimum scatter (based on a 0.1% vs. 50% occurrence of failure) is approximately 3.85. This value is largely academic at this time, as the Pressure Vessel Code remains the basis for establishing the practical typical-to-min factor for design for the near term.

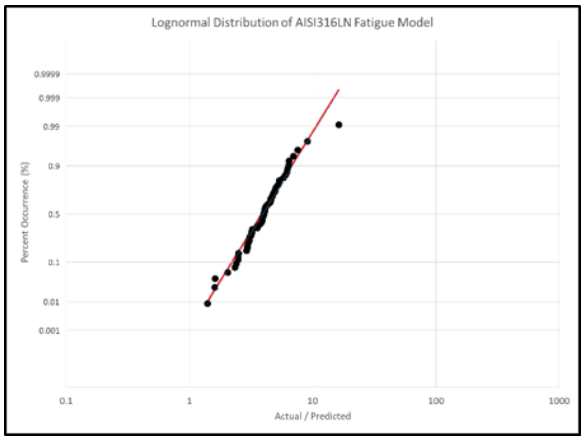

Figure 6. Lognormal Distribution of 316 A/P Data

5.5 Evaluation of Hardness Model

Application of the Hardness model (Equation 3) required a direct substitution of the original Manson Coffin coefficients and exponents with the values enumerated in the previous section.

The quality of fit at 293K (Figure 7c) is very good; both the slope and magnitude are surprisingly close to the traditional Manson Coffin model fit considering it was based on a direct calculation, and not optimization. The fits for 4K and 77K (Figures 7a, 7b) are significantly more conservative, likely because there is no hardness data available for cryogenic temperatures and the modulus does not change significantly below room temperature. Additionally, cryogenic temperatures were not the focus of their evaluation.

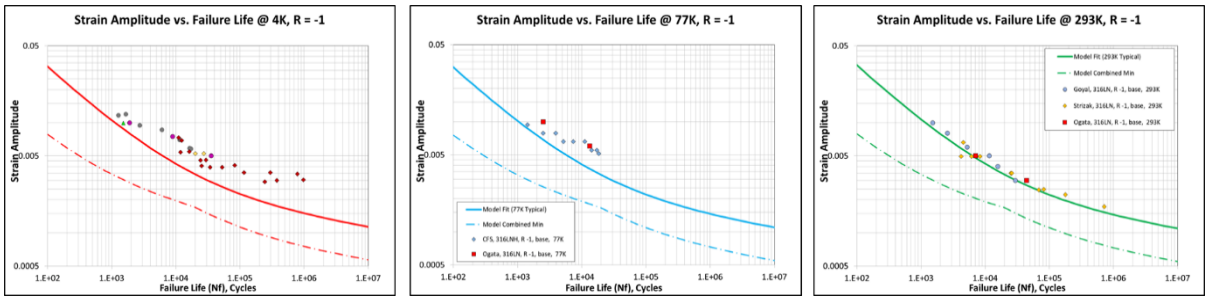

Figure 7a, b, c. Baseline Hardness Model Fit for 316 at 4K, 77K, 293K

To mitigate the apparent conservatism at lower temperatures, a simple adjustment to incorporate temperature dependency was made by multiplying the stress and strain terms in the model by their respective ultimate tensile strength (UTS) and elongation limits normalized to room temperature. Doing so offset the curves at 4K and 77K enough to more effectively match the typical fatigue behavior (Figures 8a, b, c).

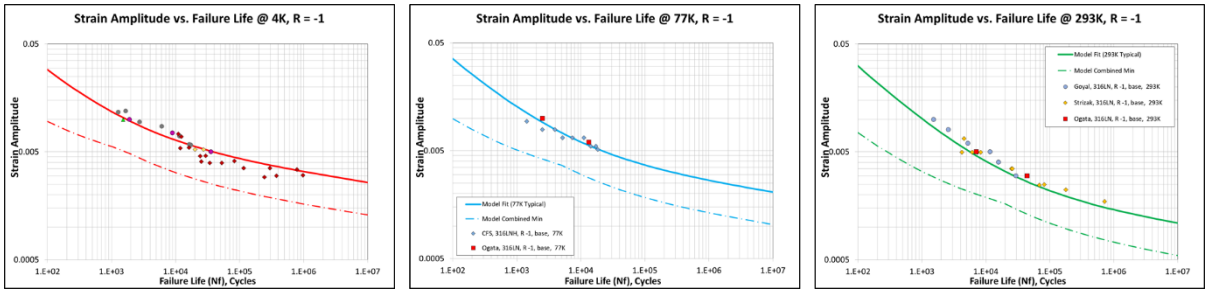

Figure 8a, b, c. Temperature-Adjusted Hardness Model Fit for 316 at 4K, 77K, 293K

Hardness-based coefficients were calculated for and applied to 297K, 700K, and 811K Inconel 718 data compiled during previous modeling work. In this case, the modulus changes noticeably as a function of temperature, which led to the conclusion that the quality of fit would be at least somewhat more consistent from one temperature to the next. Figures 9a, b, and c show the baseline model fit, i.e. without any UTS or elongation adjustment that was needed to better collapse the 316 data. Incorporating the normalization terms into the Inconel model makes the model fit slightly more conservative, but does not significantly change the overall fit. Still, it demonstrates that using the monotonic properties of Brinell hardness and elastic modulus allows us to create a series of curves that fits reasonably close – both in magnitude and curvature – to the data, and could conceivably be used as a first approximation in the absence of fatigue data.

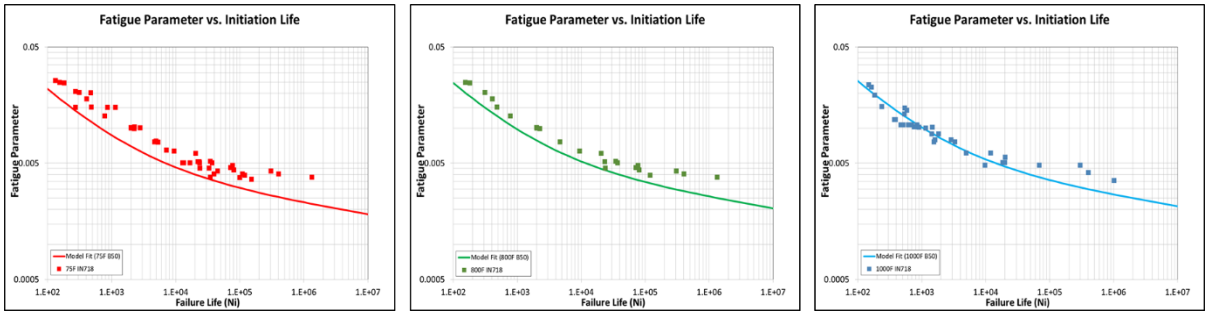

Figure 9a, b, c. Baseline Hardness Model Fit for IN718 at 297K, 700K, 811K

6. Summary

A fully reversed, temperature dependent fatigue model for the low carbon 316 stainless steel has been developed using a database created from both open source literature and recent testing from Commonwealth Fusion Systems. Though limited in scope due to the lack of non-fully reversed or notched data, much of the initial modeling work was a direct implementation of methods and practices developed during the creation of the Inconel 718 model.

Additionally, the Hartman-Glinka hardness model was applied to both 316 steel and Inconel 718 with very encouraging results. Some further work is needed in order to build a universal temperature dependency parameter into the equation, but this approach clearly shows promise in its ability to predict low cycle fatigue behavior, at least at low to intermediate temperatures, without the need for data to provide the initial foundation for identifying coefficients.

Further work, as mentioned previously, includes the incorporation of alternate stress ratio fatigue as well as notched data for at least two different geometries that will allow for the development of a proper notch adjustment factor. A fully unified model will also include higher temperature data where time dependent mechanisms are active, such as peak and valley dwell at

various hold times as well as thermal mechanical fatigue. Expansion of the hardness method to include actual hardness measurements at temperature along with evaluation of other materials using the same approach would further substantiate the efficacy of this approach.

Acknowledgments
AFMA would like to thank Commonwealth Fusion Systems for their support of our efforts and the data they provided to facilitate development of this model.

References

[1] *AISI 316 Stainless Steel Properties, SS 316 Grade Density, Composition, Yield Strength, Thermal Conductivity*. World Material. Retrieved 25 March 2025, from https://www.theworldmaterial.com/316-stainless-steel/
[2] *316 Stainless Steel: Definition, Composition, Properties, Processing, Applications, and More.* Steelpro Group. Retrieved 25 March 2025, from https://steelprogroup.com/stainless-steel/grades/grade-316/
[3] *316LN Austenitic Grade.* Stainless Structurals. Retrieved 25 March 2025, from https://www.stainless-structurals.com/download/grades-desc/316LN.pdf
[4] *316LN Stainless Steel.* Intamet Ltd. Retrieved 25 March 2025, from https://intamet.com/316ln-stainless-steel/
[5] *Stainless Steel Grade 316LN (UNS S31653)*. AZO Materials. Retrieved 25 March 2025, from https://www.azom.com/article.aspx?ArticleID=8261
[6] *ALLOY 316LN / UNS S31653 / WNR 1.4429*. FineTubes / AMETEK. Retrieved 25 March 2025, from https://www.finetubes.co.uk/products/materials/stainless-steel-tubes/alloy-316ln-uns-s31653-wnr-14429
[7] *316/316L/316LN Stainless Steel Grade Comparison.* SVF Flow Controls. Retrieved 25 March 2025, from https://svf.net/application/files/1517/0896/4416/Tech-Brief-1092-Stainless-Steel-Grade-Comparison.pdf
[8] Hamada, K., Nakajima, H., Kawano, K., Takano, K., Tsutsumi, F., & Okuno, K. 2007 Demonstration of full scale JJ1 and 316LN fabrication for ITER TF coil structure. *Fusion Engineering and Design*, **82**(5-14), 1481-1486.
[9] ASME 2021, *2021 ASME Boiler & Pressure Vessel Code VIII: Rules for Construction of Pressure Vessels Division 2: Alternative Rules*, American Society of Mechanical Engineers.
[10] Marotta, M.D., Dudzinski, D.C. 2016 August A Unified LCF Model for Conventionally Heat Treated Inconel 718. *Superalloys 2016: Proceedings of the 13th International Symposium of Superalloys* 887-895 Hoboken, NJ, USA: John Wiley & Sons, Inc
[11] Nakajima, H. 2019 Mechanical properties and material code of cryogenic structural materials for toroidal field coils used in fusion facilities. *Teion Kogaku (Online)* **54**(6), 427-436.
[12] Nakajima, H., Hamada, K., Okuno, K., Hada, K., & Tada, E. 2002 January New cryogenic steels and design approach for ITER superconducting magnet system *International Conference on Nuclear Engineering* **35987** 591-598
[13] Ogata, T., Ishikawa, K., Nagai, K., Umezawa, O., Yuri, T. 1989 Low cycle fatigue and other mechanical properties of aged 316 LN stainless steel at liquid helium temperature. *Advances in Cryogenic Engineering Materials* **36**, 1249-1255.
[14] Suzuki, K., Fukakura, J., & Kashiwaya, H. 1988 Cryogenic fatigue properties of 304L and 316L stainless steels compared to mechanical strength and increasing magnetic permeability. *Journal of Testing and Evaluation* **16**(2) 190-197
[15] Goyal, S., Veerababu, J., Sandhya, R., Laha, K., & Bhaduri, A. K. 2016 Effect of notch on low cycle fatigue behaviour of 316 LN stainless steel. *Transactions of the Indian Institute of Metals*, **69**, 1015-1022.
[16] Strizak, J. P., Tian, H., Liaw, P. K., & Mansur, L. K. 2005 Fatigue properties of type 316LN stainless steel in air and mercury. *Journal of Nuclear Materials* **343**(1-3) 134-144
[17] Manson, S.S., Halford, G. R. 2006 *Fatigue & Durability of Structural Materials* (Materials Park, Ohio, ASM International) pp 93-110
[18] Stephens, R., Fatemi, A., Stephens, R., Fuchs, H. 2001 *Metal Fatigue in Engineering* (John Wiley & Sons, New York).
[19] Botshekan, M., Degallaix, S., Desplanques, Y., & Polak, J. 1998 Tensile and LCF properties of AISI 316LN SS at 300 and 77 K. *Fatigue & Fracture of Engineering Materials & Structures*, **21**(6), 651-660.
[20] Hartman, D. 2013 Robust model for fatigue life estimation from monotonic properties data for steels *MSc Thesis* University of Waterloo